UDC 539.3

COMPUTER SIMULATION OF THE STRESS-STRAIN STATE OF THIN PLATES AND CYLINDRICAL SHELLS WITH A CIRCULAR HOLE REINFORCED BY AN INCLUSION FROM FUNCTIONALLY GRADED MATERIAL

E.L. Hart,
Doctor of Physical and Mathematical Sciences, Professor

B.I. Terokhin,
PhD student

Oles Honchar Dnipro National University,
Gagarin Ave., 72, Dnipro, 49010, Ukraine

DOI: 10.32347/2410-2547.2023.110.63-80

Computer simulation and FEM analysis of the stress-strain state of thin plates and thin-walled cylindrical shells, weakened by a circular hole in the presence of an annular inclusion of a functionally graded material (FGM) surrounding it, have been carried out. The influence of the dimensions of the FGM-inclusion and the law of change of its elastic modulus on the concentration of the parameters of the stress-strain state of plates and shells in the vicinity of the hole is studied. The distribution of stress and strain intensities in the zones of local stress concentration is obtained. It has been established that when using a radially inhomogeneous FGM-inclusion with certain mechanical properties, it is possible to reduce the stress concentration factor by more than 35%. The law of change in the modulus of elasticity of the FGM-inclusion and the width of the inclusion have a significant effect not only on the concentration of the parameters of the stress-strain state of the plate and shell, but also on the nature of the stress distribution over their surfaces. The results of a series of large-scale computational experiments show that the use of an FGM annular inclusion makes it possible to reduce the intensity of both stresses and deformations around the hole.

Keywords: elastic plate, thin-walled cylindrical shell, circular hole, annular inclusion, functionally graded material, stress-strain state, stress concentration factor, FEM analysis.

Introduction. Plates and cylindrical shells with holes are widely used in various branches of technology, in particular, rocket and space, oil and gas, energy, construction, etc. The advantage of these elements of thin-walled structures lies in their significant strength and relatively low weight. The presence of holes in plates and shells leads to a sharp increase in local stresses, which in turn affect the strength and reliability of the structure as a whole [1–4]. That is why the search for ways to reduce the stress concentration in thin-walled structures is an urgent problem in the mechanics of a deformable solid body.

Many scientific papers have been devoted to the study of the stress-strain state (SSS) of thin-walled structures with holes. Fundamental in this direction are the works of famous domestic scientists G.N. Savin, A.N. Guz and others [5, 6].

The presence of reinforcing elements or inclusions with certain mechanical properties helps to reduce the stress concentration around the holes [7–13].

The use of functionally graded materials (FGM) also makes it possible to influence the stress-strain state of thin-walled structures in order to reduce the stress concentration factor (SCF). The research uses both analytical and

numerical methods. Thus, mixed axisymmetric problems for functionally graded media were considered in [14] and their analytical solutions were obtained. In [15], using an analytical method, the stress distribution in a FGM plate with a circular hole was studied; in [16], the stress concentration in multi-wedge systems with functionally graded wedges was estimated. In [17], using the finite element method (FEM), using various isoparametric finite elements, the SCF was determined in the vicinity of a circular cut in an inhomogeneous plate under the action of a uniaxial tensile load; in [18], the SCF was determined near a circular cut in an FGM plate under the action of a biaxial tension and shift.

Taking into account the inhomogeneity of the FGM significantly increases the complexity of the mathematical model of the problem and obtaining its solution. Analytical methods for solving problems of deformation of FGM structures can be used only in some individual cases, therefore, when studying SSS structures with various inhomogeneities (holes, inclusions, etc.), it is more expedient to use numerical methods of mechanics, in particular, FEM, which, unlike analytical ones, is quite universal and effective for solving a wide class of problems [19].

In this work, as a continuation of [9, 10], computer simulation of the SSS of elastic thin plates and thin-walled cylindrical shells with a circular hole in the presence of an annular FGM inclusion around it is carried out. The FEM analysis of the influence of the dimensions of the FGM inclusion and the law of change of its elastic modulus on the SSS parameters of the plates and shells in the zone of their local concentration was carried out.

1. Problem statement. The SSS of thin elastic homogeneous isotropic plates and cylindrical shells with a centrally located circular hole and an annular radially inhomogeneous FGM inclusion is considered. Plate dimensions is $a \times b$, thickness is h, hole radius is R, inclusion radius is R_1 (Fig. 1 (a)); the length of the shells is L, diameter is d, thickness, radius of the hole and the radially inhomogeneous inclusion are the same as those of the plate (Fig. 1 (b)). The inclusion has a thickness h (located in the plane of the plate/shell), and rigid adhesion conditions are set on its boundary with the matrix. The value of the inclusion radius R_1 varies. A uniform uniaxial tensile load $p = const$ acts on the side faces of the plates and the ends of the shells, which does not lead to the appearance of plastic deformations.

In numerical calculations, several types of model materials for inclusions from FGM were selected, which have radial arbitrary elastic properties (according to linear and nonlinear laws of change in the modulus of elasticity), with the same Poisson's ratio $\nu_0 = 0.25$ and variable modulus of elasticity $E_i(r)$ $(i = \overline{1,8})$:

$$E_1(r) = 0.5E_0(2 - e^{-5(\frac{r-R}{R_1-R})}); \qquad E_2(r) = 0.5E_0(1 + \frac{r-R}{R_1-R});$$

$$E_3(r)=0.5E_0(1+e^{-5(1-\frac{r-R}{R_1-R})});\quad E_4(r)=E_0(1+0.5e^{-5(\frac{r-R}{R_1-R})});$$

$$E_5(r)=E_0(1.5-0.5\frac{r-R}{R_1-R});\quad E_6(r)=E_0(1.5-0.5e^{-5(1-\frac{r-R}{R_1-R})});$$

$$E_7(r)=\begin{cases}E_0(1+l),\ l\in[0;\ 0.5]\\ E_0(2-l),\ l\in[0.5;\ 1]\end{cases};\ E_8(r)=\begin{cases}E_0(1+\frac{1}{\tilde{h}_1}l),\ l\in\left[0;\ \tilde{h}_1\right],\\ 2E_0,\ l\in\left[\tilde{h}_1;\ \tilde{h}_1+\tilde{h}_2\right],\\ E_0(2-\frac{l-(\tilde{h}_1+\tilde{h}_2)}{\tilde{h}_3}),\ l\in\left[\tilde{h}_1+\tilde{h}_2;\ 1\right],\end{cases}\quad(1)$$

where $E_0=$ 100 GPa is the modulus of elasticity of the plate/shell, $0\le l\le 1$ is the normalized parametric distance in the radial direction from the edge of the hole (point A, Fig. 1) along the width of the inclusion $AB=h_{inc}=R_1-R$:

$$l=(r-R)/(R_1-R),\quad(2)$$

r is the distance from the center of the hole to an arbitrary point of inclusion, R and R_1 are the radii of the hole and the inclusion, respectively, and $\tilde{h}_i=h_i/h_{inc}$ $(i=\overline{1,3})$ is the dimensionless width of each of the three characteristic zones of the FGM inclusion $h_{inc}=\sum_{i=1}^{3}h_i$ (Fig. 2 (d)).

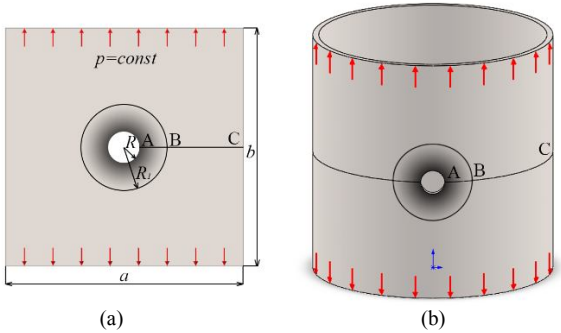

(a) (b)

Fig. 1. Geometry and loading scheme of the plate (a) and shell (b) with radially inhomogeneous inclusion

The form of dependences for model materials (1) with $E_i(r)$ $(i=1,\ 4)$ is similar to [15]. Dependences (1) with $E_i(r)$ $(i=\overline{1,\ 3})$ correspond to "soft", and with $E_i(r)$ $(i=\overline{4,\ 8})$ more "hard" than the main material of the plate/shell, inclusion.

On Fig. 2 shows the corresponding graphical representations of the laws of change in the elastic modulus of the FGM-inclusion for "soft" (Fig. 2 (a)) and "hard" (Fig. 2 (b) – Fig. 2 (d)) inclusions. Lines 1 – 8 correspond to dependencies (1) for $E_i(r)$ $(i=\overline{1,8})$. Here and below in the figures, the abscissa shows the normalized parametric distance (2), $0 \le l \le 1$ in the radial direction from the edge of the hole along the width of the inclusion.

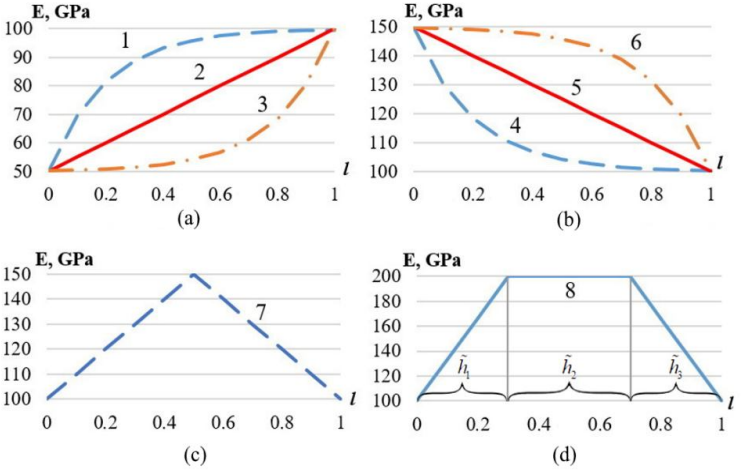

Fig. 2. The laws of change in the modulus of elasticity of FGM-inclusions: "soft" (a), "hard" (b)–(d)

Further, when this does not cause confusion, each of the eight variants of FGM inclusions (1) with a variable modulus of elasticity $E_i(r)$ $(i=\overline{1,8})$ will be denoted by the corresponding index according to Fig. 2.

For definiteness, it was assumed that the plate is square, and the length of the shells L is equal to the side of the plate.

On Fig. 2 (d) we have a graphical representation of three characteristic zones of the law of change in the modulus of elasticity of the FGM-inclusion (1) from $E_i(r)$ $(i=8)$: 1) a zone of growth in width $\tilde{h}_1$; 2) a zone of constant (fixed) value width $\tilde{h}_2$; 3) a zone of decrease in the modulus of elasticity with a width of $\tilde{h}_3$.

2. Mathematical Model of the Problem. In the variational formulation, the original problem for a cylindrical shell leads to the minimization of the functional of the total potential energy of the deformation of the system [1]:

$$F=\sum_{s=1}^{n+1}\left\{\frac{1}{2}\int\limits_{\Omega_s}\frac{E_s(x,y)h}{(1-\nu_s{}^2)}\left[\left(\frac{\partial u}{\partial x}\right)^2+\left(\frac{\partial v}{\partial y}+\frac{w}{\tilde{R}}\right)^2+2\nu_s\left(\frac{\partial u}{\partial x}\right)\left(\frac{\partial v}{\partial y}+\frac{w}{\tilde{R}}\right)+\frac{1-\nu_s}{2}\times\right.\right.$$

$$\times\left(\frac{\partial u}{\partial y}+\frac{\partial v}{\partial x}\right)^2\Bigg]dxdy+\frac{1}{2}\int\limits_{\Omega_s}\frac{E_s(x,y)h^3}{12(1-\nu_s{}^2)}\Bigg[\left(\frac{\partial^2 w}{\partial x^2}\right)^2+\left(\frac{\partial^2 w}{\partial y^2}+\frac{w}{\tilde{R}}\right)^2+2\nu_s\left(\frac{\partial^2 w}{\partial x^2}\right)\times$$

$$\times\left(\frac{\partial^2 w}{\partial y^2}+\frac{w}{\tilde{R}}\right)+2(1-\nu_s)\left(\frac{\partial^2 w}{\partial x\partial y}\right)^2\Bigg]dxdy\Bigg\}-\int\limits_{\gamma}\left(p_x u+p_y v+p_z w\right)\,dxdy,$$

where $u(x,y)$, $v(x,y)$, $w(x,y)$ are the projections of the displacement vector on the axes Ox, Oy and Oz, respectively; h is shell thickness; $\tilde{R}$ is the radius of the shell; $E_s(x,y)$, $\nu_s\,60^\circ$ are modulus of elasticity and Poisson's ratio of the shell Ω_1 (matrix) $(s=1)$ material and inclusion Ω_s $(s=\overline{2,n+1},\ n$ is the number of inclusions); $\Omega=\bigcup_{s=1}^{n+1}\Omega_s$ is domain of definition of variables x and y; γ is the boundary of the region Ω along which the external intensity load $P(x,y)=(p_x(x,y),\ p_y(x,y),\ p_z(x,y))^T$ is applied. In the case of a uniaxial tensile load $p_x(x,y)=p_z(x,y)=0$, $p_y(x,y)=p=const$.

In the case of a plate, we arrive at the problem of minimizing the functional of the total potential strain energy of a system of this type [20]:

$$F=\sum_{s=1}^{n+1}\Bigg\{\frac{1}{2}\int\limits_{\Omega_s}\frac{E_s(x,y)h}{(1-\nu_s{}^2)}\Bigg[\left(\frac{\partial u}{\partial x}\right)^2+\left(\frac{\partial v}{\partial y}\right)^2+2\nu_s\left(\frac{\partial u}{\partial x}\right)\left(\frac{\partial v}{\partial y}\right)+$$

$$+\frac{1-\nu_s}{2}\left(\frac{\partial u}{\partial y}+\frac{\partial v}{\partial x}\right)^2\Bigg]dxdy\Bigg\}-\int\limits_{\gamma}\left(p_x u+p_y v\right)\,dxdy.$$

The stated variational problems are solved using the FEM using isoparametric triangular six-node Lagrangian finite elements of the second degree, while the unknown displacement functions inside each finite element are approximated by a quadratic polynomial. In the areas of stress concentration, an adaptive mesh was used (Fig. 3) with a refinement factor equal to 10. The convergence of the FEM in the case of using flat finite elements for thin-walled shells is ensured here by mesh refinement. The use of a finer grid leads to an increase in the accuracy of approximation of the shell surface by the geometry of the inscribed polyhedron.

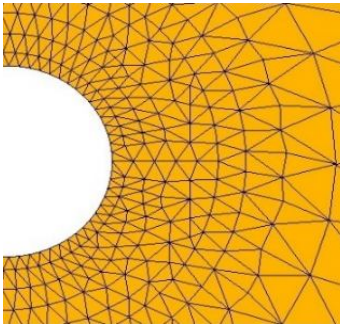

Fig. 3. Fragment of adaptive finite element mesh

3. Analysis of numerical results. Computational experiments were carried out on a PC with an Intel Core i7-10700F processor, a clock frequency of 2.9-4.8 GHz, 32 GB RAM, x64 system capacity. The average number of finite elements in the calculation of plates is 2126, the number of nodes is 4408; when calculating shells 6372 and 13002, respectively.

Numerical results were obtained for: 1) square plates with the following geometric parameters: $h = 0.005\,\text{m}$, $a = b = 0.2\,\text{m}$, $R = a/20$; 2) cylindrical shells with parameters: $L = d = a$, $h = 0.005\,\text{m}$, $R = d/10$. Tensile load in both cases $p = 10\,\text{MPa}$.

The radius R_1 of the annular radially inhomogeneous FGM-inclusion around the hole was varied with a step of R, while the width of the FGM-inclusion was $h_{inc} = R, 2R, ..., 9R$.

3.1. Plates with radially inhomogeneous inclusions. As a result of the computational experiments, using the FEM, the distribution of stress and strain intensities in the plate was obtained, and the SCF was calculated for uniaxial tension of the plate with "soft" and "hard" FGM-inclusions with the inclusion width R and $2R$. The results for “soft” inclusions (Fig. 2 (a)) are shown in Table 1, for "hard" inclusions (Fig. 2 (b), Fig. 2 (c)) are given in Table 2. In Fig. 4 illustrates the nature of the distribution of relative stresses σ_y/p in the plate along the width of the inclusion in section AB at $h_{inc} = 2R$ for “soft” radially inhomogeneous inclusions (1) from $E_i(r)$ $(i = \overline{1, 3})$ (Fig. 4 (a)) and “hard” from $E_i(r)$ $(i = \overline{4, 7})$ (Fig. 4 (b), Fig. 4 (c)).

As can be seen from Fig. 4 (c), in the case of an FGM inclusion (1) from $E_i(r)$ $(i = 7)$, the maximum stresses in the vicinity of the hole and the relative stresses σ_y/p in the section AB in the interval $l \in [0.7, 1]$ along the width of the inclusion turn out to be smaller than in the plate without inclusions.

For the purpose of comparative analysis, a calculation was made for a homogeneous plate with a circular hole without inclusion. Received SCF=3.05; the maximum value of the strain intensity in this case is $\varepsilon_i^{\max} = 2.13 \times 10^{-4}$, which is in good agreement with the results of [5].

The patterns of distribution of stress and strain intensities in a plate with an FGM-inclusion (1) with the law of change in the elastic modulus $E_i(r)$ $(i = 7)$ are shown in Fig. 5.

Therefore, the use of FGM inclusions around the hole leads to a smooth distribution of stresses in the matrix without jump-like perturbations, in contrast to a homogeneous inclusion. The width of FGM inclusions affects the nature of the stress distribution: the larger the width of the inclusion, the smoother the redistribution of stresses in the matrix.

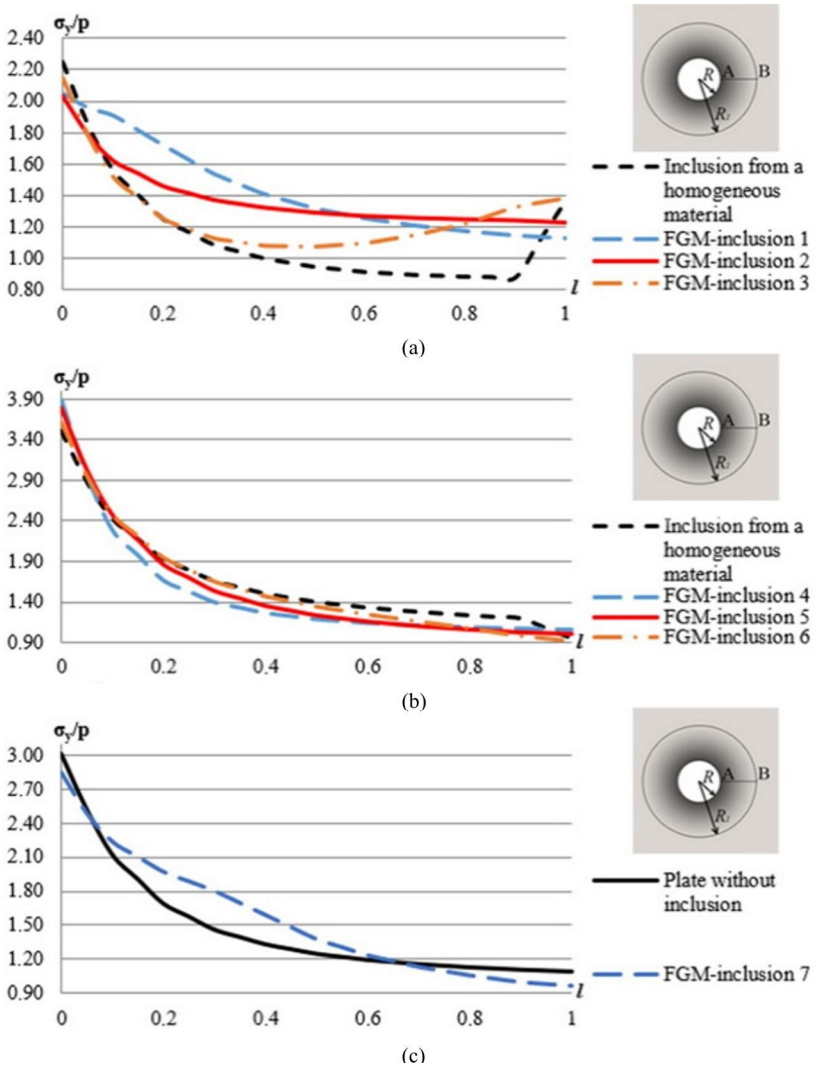

Fig. 4. Distribution of relative stresses σ_y/p in the plate along the width of the inclusion in the section AB at $h_{inc}=2R$ for "soft" (a) and "hard" (b), (c) FGM-inclusions

The best option among those considered (Fig. 2 (a) – Fig. 2 (c)) turned out to be the case of FGM-inclusion 7, in which the elastic modulus increases radially from the edge of the hole to its middle in the direction of the periphery, and then decreases (Fig. 2 (c)). In this case, not only does the strength of the plate as a whole increase, but it is also possible to reduce the concentration of stresses and strains around the hole by ~7% and ~9%, respectively. This confirms the expediency of using FGM-inclusions of this type and opens up prospects for further searches for their optimal parameters.

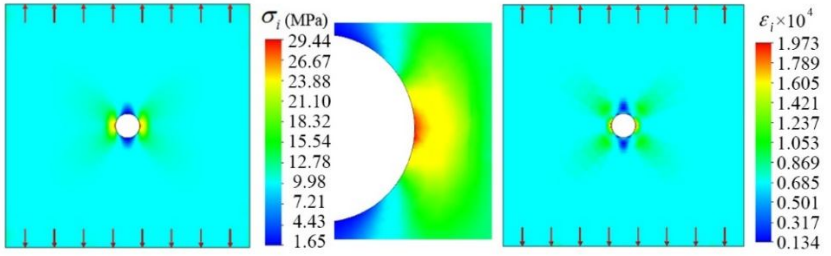

(a) (b) (c)

Fig. 5. SSS components of a plate with FGM-inclusion 7 at $h_{inc}=R$: stress intensity (a), stress intensity in the vicinity of the hole (b), strain intensity (c)

It can be seen from Table 1 that in the case of a radially inhomogeneous inclusion of width $2R$ from an FGM type with $E_i(r)$ $(i=\overline{1,3})$ maximum deformations and the SCF in a plate with a hole is less than in the presence of a "soft" homogeneous inclusion: for FGM-inclusion 2, the difference in maximum deformations is ~1.6 times, for FGM-inclusions 1 is by ~2.5 times; the decrease in SCF is 7% in both cases. Consequently, when using "soft" inclusions, the SCF decreases.

Table 1

Stress concentration factor and corresponding deformations in a plate with "soft" FGM-inclusion at $h_{inc}=2R$

The task	SCF	δ_1, %	$\varepsilon_i^{\max}\times 10^4$	δ_2, %
Inclusion from a homogeneous material, $E_{inc}=0.5E_0$	2.25	-26.4	3.14	+47.4
FGM-inclusion 1	2.05	-33.1	2.54	+19.3
FGM-inclusion 2	2.03	-33.7	2.75	+29.1
FGM-inclusion 3	2.11	-30.9	2.92	+37.1

Here, δ_1 and δ_2 are the deviation of the SCF and the maximum value of the strain intensity $\varepsilon_i^{\max}$ from the corresponding value for a plate with a circular hole without an inclusion [5].

The use of "hard" inclusions increases the strength of the structure as a whole. In the case of FGM-inclusions (1) with $E_i(r)$ $(i=\overline{4,6})$, there is some increase in the SCF in the vicinity of the hole, but in the case of FGM-inclusions with $E_i(r)$ $(i=7)$, both stresses and strains around the hole decrease compared to a plate without inclusions (Table 2).

The results of studies carried out in [9] for the problem with an FGM-inclusion (1) from $E_i(r)$ $(i=8)$ (Fig. 2 (d)) indicate that the width h_2 of the central zone of an FGM-inclusion of this type has the greatest influence on the SCF value. It has been established that the smaller the size of the first zone

(h_1) of the FGM-inclusion, the smaller the SCF value. To identify the rational parameters of the first zone of the FGM-inclusion 8 (Fig. 2 (d)), we will carry out calculations with varying values h_1 and h_2 with a constant width of the third zone h_3 (Table 3).

Table 2

Stress concentration factor and corresponding deformations in a plate with "hard" FGM-inclusion at $h_{inc} = 2R$

The task	SCF	δ_1, %	$\varepsilon_i^{\max} \times 10^4$	δ_2, %
Inclusion from a homogeneous material, $E_{inc} = 1.5E_0$	3.51	15.1	1.63	-23.5
FGM-inclusion 4	3.90	27.9	1.89	-11.3
FGM-inclusion 5	3.79	24.3	1.77	-16.9
FGM-inclusion 6	3.62	18.7	1.68	-21.1
FGM-inclusion 7	2.84	-6.9	1.93	-9.4

Table 3

Variants of FGM-inclusions depending on the width of the zones h_i ($h_{inc} = 3R,\ 4R$)

Width of FGM-inclusion zones / Inclusion type	h_1	h_2	h_3
FGM-inclusions 1.1	R	R	R
FGM-inclusions 1.2	$0.75R$	$1.25R$	R
FGM-inclusions 1.3	$0.5R$	$1.5R$	R
FGM-inclusions 1.4	$0.25R$	$1.75R$	R
FGM-inclusions 1.5	R	$2R$	R
FGM-inclusions 1.6	$0.75R$	$2.25R$	R
FGM-inclusions 1.7	$0.5R$	$2.5R$	R
FGM-inclusions 1.8	$0.25R$	$2.75R$	R

Here, FGM-inclusions 1.1–1.4 are $3R$ wide, and FGM-inclusions 1.5–1.8 are $4R$ wide.

The results of the computational experiments performed using the FEM for plates with FGM-inclusions (1) from $E_i(r)$ $(i = 8)$ (Fig. 2 (d)) of different widths are summarized in Table 4.

Table 4 shows that for inclusions with a width of $3R$ and $4R$, the smallest SCF was obtained in the cases of FGM-inclusion 1.3 and FGM-inclusion 1.7, respectively, when $h_1 = 0.5R$. If we compare the cases of FGM-inclusions when $h_1 = 0.5R$ and $h_1 = R$, the SCF values differ by ~1%. Therefore, for convenience, we will continue to perform calculations when $h_1 = R$.

Table 4

Stress concentration factor and corresponding deformations in a plate with FGM-inclusion

The task	SCF	δ_1, %	$\varepsilon_i^{\max} \times 10^4$	δ_2, %
FGM-inclusions 1.1	2.39	-21.6	1.60	-24.9
FGM-inclusions 1.2	2.36	-22.6	1.57	-26.3
FGM-inclusions 1.3	2.35	-23.0	1.53	-28.2
FGM-inclusions 1.4	2.55	-16.4	1.48	-30.5
FGM-inclusions 1.5	2.23	-26.9	1.50	-29.6
FGM-inclusions 1.6	2.21	-27.5	1.47	-31.0
FGM-inclusions 1.7	2.20	-27.9	1.43	-32.9
FGM-inclusions 1.8	2.41	-21.0	1.39	-34.7

Let us find out how the SCF changes for different variants of the width of the inclusion at fixed values h_1, h_3 and a variable value h_2 of the FGM-inclusion (1) from $E_i(r)$ $(i=8)$ (Fig. 2 (d)) (Table 5).

Table 5

Variants of FGM-inclusions depending on the width of the zones h_i $(h_{inc}=3R,\ 4R,...,9R)$

Width of FGM-inclusion zones / Inclusion type	h_1	h_2	h_3
FGM-inclusions 2.1	R	R	R
FGM-inclusions 2.2	R	$2R$	R
FGM-inclusions 2.3	R	$3R$	R
FGM-inclusions 2.4	R	$4R$	R
FGM-inclusions 2.5	R	$5R$	R
FGM-inclusions 2.6	R	$6R$	R
FGM-inclusions 2.7	R	$7R$	R

In the case of an FGM-inclusion 2.7 ($h_{inc}=9R$), its radius R_1 is equal to half the width of the plate. In this case, it was assumed that the entire plate was made of FGM.

The results of a series of computational experiments using the FEM for plates with FGM-inclusions (1) from $E_i(r)$ $(i=8)$ (Fig. 2 (d)) of different widths $(h_{inc}=3R,\ 4R,...,9R)$ are summarized in Table 6.

The presence of an annular FGM-inclusion (1) with a given law of change in the elastic modulus $E_i(r)$ $(i=8)$ makes it possible to reduce the SCF value in the plate by ~21%–38%, and the maximum deformations by ~25%–40% (Table 6). Analyzing the results of calculations in the presence of FGM-inclusions of different widths, we find that the larger the width of the

inclusion, the smaller the values of SCF and deformations in the plate. The smallest SCF value among the variants under consideration was obtained in the case of FGM-inclusion 2.6 ($h_1 = h_3 = R$, $h_2 = 6R$).

Table 6

Stress concentration factor and corresponding deformations in a plate with FGM-inclusion

The task	SCF	δ_1, %	$\varepsilon_i^{\max} \times 10^4$	δ_2, %
FGM-inclusions 2.1	2.39	-21.6	1.60	-24.9
FGM-inclusions 2.2	2.23	-26.9	1.50	-29.6
FGM-inclusions 2.3	2.10	-31.1	1.41	-33.8
FGM-inclusions 2.4	1.99	-34.8	1.34	-37.1
FGM-inclusions 2.5	1.93	-36.7	1.30	-39.0
FGM-inclusions 2.6	1.90	-37.7	1.28	-39.9
FGM-inclusions 2.7	1.93	-36.7	1.30	-39.0

On Fig. 6 shows the graphs of the distribution of relative stresses σ_y / p in the characteristic cross section AC of a plate with an FGM-inclusion (1) from $E_i(r)$ $(i = 8)$ for various options for the width h_2 of the second zone of the FGM-inclusion $h_2 = R;\ 2R;...,7R$ (see Table 3). The abscissa shows the normalized parametric distance $0 \le l_1 \le 1$ in the radial direction from the hole edge (point A, Fig. 1 (a)) along the plate cross section $AC = (a - 2R)/2$: $l_1 = (r - R) / (\frac{a}{2} - R)$, r is the distance from the center of the hole to an arbitrary point of the segment AC .

As can be seen from Fig. 6, when using FGM-inclusions of different widths, a redistribution of stresses occurs in the cross section AC associated with the width h_2 of the central zone of the FGM-inclusion: the larger the value of h_2, the lower the stress σ_y / p in the section AC ; in the transition from the second to the third zone, for each FGM-inclusion 2.4–2.7, the stresses σ_y / p decrease.

Consequently, by setting a certain law of change in the elastic modulus of the inclusion, it is possible to influence the magnitude of the SCF and, in general, the distribution of stresses in the plate.

As an example, in Fig. 7 shows the distribution of stress intensity σ_i in a plate with a circular hole and FGM-inclusion 2.6 ($h_1 = h_3 = R,\ h_2 = 6R$).

On Fig. 8 illustrates the qualitative nature of the difference in the distribution of strain intensities in a homogeneous plate and in a plate with a radially inhomogeneous inclusion (1) from $E_i(r)$ $(i = 8)$ along the radius $R_1 = 8R$ ($h_1 = h_3 = R,\ h_2 = 6R$).

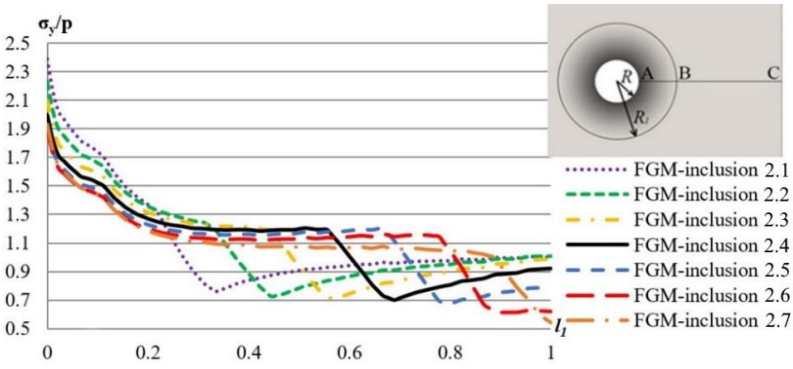

Fig. 6. Distribution of relative stresses σ_y / p in a plate with an FGM-inclusion in the cross section AC in the case $h_2 = R,\ 2R,...,7R$

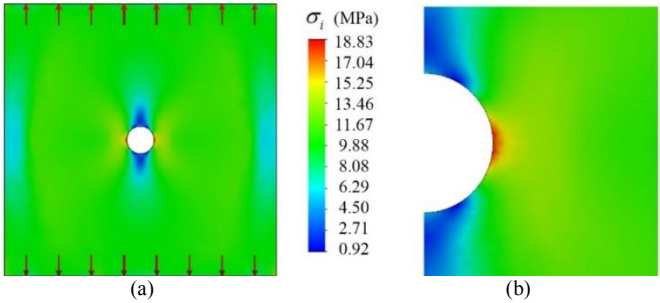

(a) (b)

Fig. 7. Stress intensity distribution in a plate with FGM-inclusion 2.6 (a), a fragment of the distribution σ_i around the hole (b)

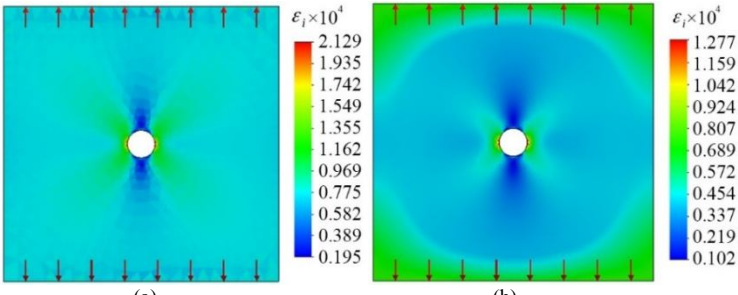

(a) (b)

Fig. 8. Strain intensity distribution ε_i in a homogeneous plate (a) and in a plate with an FGM-inclusion 2.6 (b)

3.2. Cylindrical shells with radially inhomogeneous inclusions. Next, let us consider the effect on the SCF value of the presence of FGM-inclusions with a given law of change in the elastic modulus in the radial direction around a circular hole in a cylindrical thin-walled shell.

The results of calculations for a shell with FGM-inclusions (1) from $E_i(r)$ $(i=8)$ (Fig. 2 (d)) with varying values h_1, h_2 and a constant width of the third zone h_3 (see Table 3) are given in Table 7.

Table 7

Stress concentration factor and corresponding deformations in a cylindrical shell with an FGM-inclusion

The task	SCF	δ_1, %	$\varepsilon_i^{\max}\times10^4$	δ_2, %
FGM-inclusions 1.1	2.49	-23.9	1.66	-27.2
FGM-inclusions 1.2	2.42	-26.0	1.59	-30.3
FGM-inclusions 1.3	2.41	-26.3	1.55	-32.0
FGM-inclusions 1.4	2.50	-23.5	1.51	-33.8
FGM-inclusions 1.5	2.32	-29.1	1.55	-32.0
FGM-inclusions 1.6	2.25	-31.2	1.48	-35.1
FGM-inclusions 1.7	2.24	-31.5	1.45	-36.4
FGM-inclusions 1.8	2.30	-29.7	1.39	-39.0

Here, as in the case of plates, the smallest SCF was obtained for FGM-inclusions of widths $3R$ and $4R$ in the case of $h_1=0.5R$. If we compare the cases of FGM-inclusions with $h_1=0.5R$ and $h_1=R$, then the SCF values differ by ~2%. Therefore, further we will consider the rational parameter of the first zone $h_1=R$.

Let us find out how the SCF changes in the shell for different values R_1 $(h_{inc}=3R,\ 4R,...,9R)$ (Table 5) at fixed values h_1, h_3 and a variable value h_2 of the FGM-inclusion (1) from $E_i(r)$ $(i=8)$ (Fig. 2 (d)). The results of a series of computational experiments are summarized in Table 8.

Table 8

Stress concentration factor and corresponding deformations in a cylindrical shell with an FGM-inclusion

The task	SCF	δ_1, %	$\varepsilon_i^{\max}\times10^4$	δ_2, %
FGM-inclusions 2.1	2.49	-23.9	1.66	-27.2
FGM-inclusions 2.2	2.32	-29.1	1.55	-32.0
FGM-inclusions 2.3	2.20	-32.7	1.46	-36.0
FGM-inclusions 2.4	2.11	-35.5	1.41	-38.2
FGM-inclusions 2.5	2.07	-36.7	1.39	-39.0
FGM-inclusions 2.6	2.06	-37.0	1.38	-39.5
FGM-inclusions 2.7	2.11	-35.5	1.41	-38.2

Here, δ_1 and δ_2 are the deviation of the SCF and the maximum value of the strain intensity $\varepsilon_i^{\max}$ from the corresponding value for a thin-walled cylindrical shell with a circular hole without an inclusion [6].

From Table 8 it can be seen that the presence of a radially inhomogeneous ring inclusion with a given law of change in the elastic modulus leads to a decrease in the SCF value in the shell by ~24%–37%, and maximum deformations by ~27%–39%. As in the case with plates, the FGM-inclusion 2.6 ($h_1 = h_3 = R,\ h_2 = 6R$) turned out to be the best of the considered options for the shell in terms of reducing the SCF.

As can be seen from Fig. 9, the distribution of relative stresses σ_y / p over the surface of the shell (in section AC) for FGM-inclusions of different widths is similar to the case for plates. The normalized parametric distance $0 \le l_2 \le 1$ from the edge of the hole (point A, Fig. 1 (b)) along the arc $AC = (\pi d - 4R)/4$ is plotted along the abscissa.

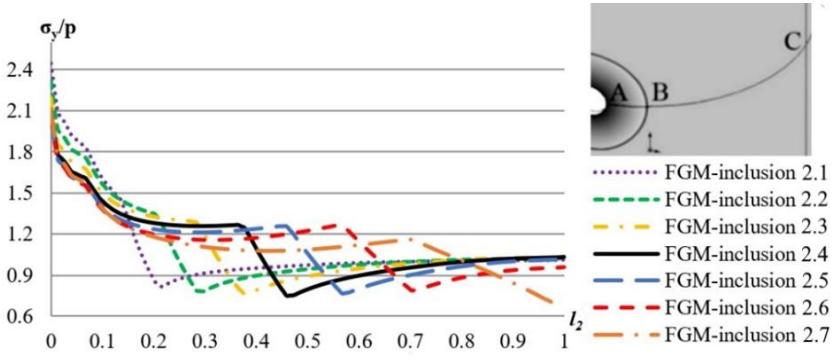

Fig. 9. Distribution of relative stresses σ_y / p in a shell with an FGM-inclusion in the cross section AC in the case $h_2 = R,\ 2R, ..., 7R$

On Fig. 10 and Fig. 11 illustrates a qualitative picture of the distribution of stress σ_i and strain ε_i intensities in a cylindrical shell with a circular hole and an annular FGM-inclusion 2.6 ($h_1 = h_3 = R,\ h_2 = 6R$), respectively.

Conclusions. Based on a series of large-scale computational experiments using the FEM, modeling and analysis of the influence of a radially inhomogeneous ring inclusion on the stress concentration around a circular hole in thin plates and cylindrical shells is carried out. The results of computer simulation and numerical study of the influence of the geometric characteristics of the FGM-inclusion and the law of change of its elastic modulus in the radial direction on the concentration of SSS parameters around the hole of the plate-shell structural elements showed that in the presence of FGM-inclusions with certain mechanical properties and geometric

characteristics, it is possible to reduce the SCF and the corresponding strain intensity in the vicinity of the hole by more than 35%.

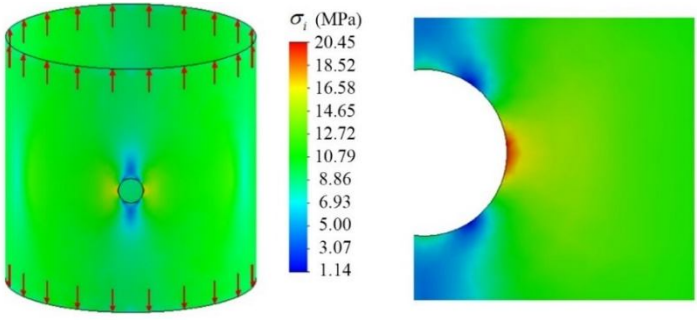

(a) (b)

Fig. 10. Stress intensity distribution in the shell with FGM-inclusion 2.6 (a), distribution fragment σ_i around the hole (b)

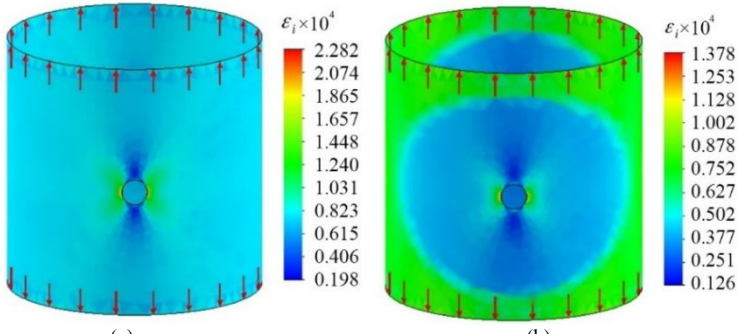

(a) (b)

Fig. 11. Strain intensity distribution ε_i in a homogeneous shell (a) and in the shell with FGM-inclusion 2.6 (b)

Therefore, the use of annular reinforcements of circular holes in the form of FGM inclusions in plates and cylindrical shells with holes is appropriate. It allows one to influence not only the nature of the distribution, but also the magnitude of stress and strain intensities in the zones of local concentration of SSS parameters.

It is promising to search for rational parameters of FGM-inclusions, to find their types and configurations from the point of view of the influence on the decrease in the concentration of SSS parameters of plates and shells with different holes.

REFERENCES

1. *Avdonin A.S.* Prikladnie metodi rascheta obolochek i tonkostennih konstrukcii (Applied methods for calculating shells and thin-walled structures). – M., 1969. – 402 p.

2. *Bazhenov V., Perelmuter A., Vorona Yu.* Structural mechanics and theory of structures. History essays. – LAP LAMBERT Academic Publishing. Beau Bassin, Mauritius, 2017. – 580 p.
3. *Lukianchenko O., Kostina O.* The finite element metod in problems of the thin shells theory. – LAP LAMBERT Academic Publishing, Beau Bassin, Mauritius, 2019. – 134 p.
4. *Peterson R.* Koeffitsiyenty kontsentratsii napryazheniy (Stress concentration factors). – M., 1977. – 302 p.
5. *Savin G.N.* Raspredeleniye napryazheniy okolo otverstiy (Stress distribution around holes). – Kyiv, 1968. – 888 p.
6. *Guz A.N., Chernyshenko I.S., Chekhov Val. N. et al.* Metody rascheta obolochek. V 5 t. T. 1. Teoriya tonkikh obolochek, oslablennykh otverstiyami (Shell calculation methods. In 5 vols. Vol. 1. Theory of thin shells weakened by holes). – Kyiv, 1980. – 636 p.
7. *Gudramovich V.S., Gart É.L., Strunin K.A.* Modeling of the behavior of plane-deformable elastic media with elongated elliptic and rectangular inclusions // Materials Science. – 2017. – Vol. 52, Iss. 6. – P. 768–774.
8. *Hart E.L., Hudramovich V.S.* Computer simulation of the stress-strain state of plates with reinforced elongate rectangular holes of various orientations // Strength of materials and theory of structures: Scientific-and-technical collected articles. – Kyiv: KNUBA, 2022. – Iss. 108. – P. 77–86.
9. *Hart E.L., Hudramovich V.S., Terokhin B.I.* Vplyv vklyuchennya iz funktsional′no-hradiyentnoho materialu na kontsentratsiyu napruzhen′ v tonkykh plastynakh ta tsylindrychnykh obolonkakh z kruhovym otvorom (Effect of a functionally graded material inclusion on the stress concentration in thin plates and cylindrical shells with a circular opening) // Tekhnichna mekhanika. – 2022. – № 4. – P. 67–78.
10. *Hart E.L., Terokhin B.I.* Computer simulation of the stress-strain state of the plate with circular hole and functionally graded inclusion // Journal of Optimization, Differential Equations and their Applications. – 2021. – Vol. 29, Iss. 1. – P. 42–53.
11. *Hart E.L., Terokhin B.I.* Vybir ratsional′nykh parametriv pidkriplyuyuchykh elementiv pry komp″yuternomu modelyuvanni povedinky tsylindrychnoyi obolonky z dvoma pryamokutnymy otvoramy (Choice of rational parameters of reinforcement elements in computer simulation of behavior of a cylindrical shell with two rectangular holes) // Problemy obchyslyuval′noyi mekhaniky i mitsnosti konstruktsiy: zb. nauk. prats′. – Dnipro: Lira, 2019. – Vol. 30. – P. 19–32.
12. *Hudramovych V.S., Hart E.L., Marchenko O.A.* Vplyv formy pidkriplen′ na napruzheno-deformovanyy stan tsylindrychnoyi obolonky z vydovzhenymy pryamokutnymy otvoramy (About the influence of the form of reinforcement on the stress-strain state of a cylindrical shell with elongated rectangular holes) // Problemy obchyslyuval′noyi mekhaniky i mitsnosti konstruktsiy: zb. nauk. prats′. – Dnipro, 2017. – Vol. 27. – P. 52–64.
13. *Hudramovich V.S., Hart E.L., Marchenko O.A.* Reinforcing inclusion effect on the stress concentration within the spherical shell having an elliptical opening under uniform internal pressure // Strength of Materials. – 2021. – Vol. 52, No. 6. – P. 832–842.
14. Analiticheskiye resheniya smeshannykh osesimmetrichnykh zadach dlya funktsional'no-gradiyentnykh sred (Analytical solutions of mixed axisymmetric problems for functionally graded media) / S.M. Aizikovich [et al.]. – M., 2011. – 192 p.
15. *Yang Q., Gao C.-F., Chen W.* Stress analysis of a functional graded material plate with a circular hole // Arch. Appl. Mech. – 2010. – Vol. 80. – P. 895–907.
16. *Linkov A., Rybarska-Rusinek L.* Evaluation of stress concentration in multi-wedge systems with functionally graded wedges // Intern. J. Engng Sci. – 2012. – Vol. 61. – P. 87–93.
17. *Kubair D.V., Bhanu-Chandar B.* Stress concentration factor due to a circular hole in functionally graded panels under uniaxial tension // Intern. J. Mech. Sci. – 2008. – Vol. 50. – P. 732–742.
18. *Mohammadi M., Dryden J. R., Jiang L.* Stress concentration around a hole in a radially inhomogeneous plate // Intern. J. Solids Structures. – 2011. – Vol. 48. – P. 483–491.
19. *Zienkiewicz O.C, Taylor R.L.* The finite element method for solid and structural mechanics. – New York: Elsevier, 2005. – 632 p.
20. *Washizu K.* Variational Methods in Elasticity and Plasticity. – Oxford-New York: Pergamon Press, 1975. – 420 p.

Стаття надійшла 11.03.2023

Гарт Е.Л., Терьохін Б.І.

КОМП'ЮТЕРНЕ МОДЕЛЮВАННЯ НАПРУЖЕНО-ДЕФОРМОВАНОГО СТАНУ ТОНКИХ ПЛАСТИН ТА ЦИЛІНДРИЧНИХ ОБОЛОНОК З КРУГОВИМ ОТВОРОМ, ПІДКРІПЛЕНИМ ВКЛЮЧЕННЯМ ІЗ ФУНКЦІОНАЛЬНО-ГРАДІЄНТНОГО МАТЕРІАЛУ

Здійснено комп'ютерне моделювання та скінченноелементний аналіз напружено-деформованого стану тонких пластин і тонкостінних циліндричних оболонок, послаблених круговим отвором за наявності оточуючого його кільцевого включення із функціонально-градієнтного матеріалу (ФГМ). Досліджено вплив розмірів ФГМ-включення та закону змінення його модуля пружності на концентрацію параметрів напружено-деформованого стану пластин і оболонок в околі отвору. Отримано розподіл інтенсивностей напружень і деформацій в зонах локальної концентрації напружень. Встановлено, що за використання радіально неоднорідного ФГМ-включення з певними механічними властивостями можна зменшити коефіцієнт концентрації напружень більш ніж на 35%. Закон змінення модуля пружності ФГМ-включення та ширина включення суттєво впливають не тільки на величину концентрації параметрів напружено-деформованого стану пластини та оболонки, а й на характер розподілу напружень по їх поверхням. Результати проведеної серії широкомасштабних обчислювальних експериментів показують, що використання кільцевого включення із ФГМ дає змогу знизити інтенсивності як напружень, так і деформацій навколо отвору.

Keywords: пружна пластина, тонкостінна циліндрична оболонка, круговий отвір, кільцеве включення, функціонально-градієнтний матеріал, напружено-деформований стан, коефіцієнт концентрації напружень, скінченноелементний аналіз.

УДК 539.3
Гарт Е.Л., Терьохін Б.І. **Комп'ютерне моделювання напружено-деформованого стану тонких пластин та циліндричних оболонок з круговим отвором, підкріпленим включенням із функціонально-градієнтного матеріалу** // Опір матеріалів і теорія споруд: наук.-тех. збірн. – К.: КНУБА, 2023. – Вип. 110. – С. 63-80. – Англ.
Із застосуванням методу скінченних елементів проведено комп'ютерне моделювання впливу механічних і геометричних параметрів підкріплювальних елементів у вигляді кільцевих включень із функціонально-градієнтного матеріалу на концентрацію напружень у тонких пластинах і циліндричних оболонках із круговим отвором.
Табл. 8. Іл. 11. Бібліогр. 20 назв.

UDC 539.3
Hart E.L., Terokhin B.I. **Computer simulation of the stress-strain state of thin plates and cylindrical shells with a circular hole reinforced by an inclusion from functionally graded material** // Strength of Materials and Theory of Structures: Scientific-and-technical collected articles. – Kyiv: KNUBA, 2023. – Issue 110. – P. 63-80. – Engl.
On the basis of the finite element method, computer simulation of the influence of mechanical and geometric parameters of reinforcing elements in the form of ring inclusions from a functionally graded material on the stress concentration in thin plates and cylindrical shells with a round hole was carried out.
Tabl. 8. Fig. 11. Ref. 20.

Автор (науковий ступень, вчене звання, посада): *доктор фізико-математичних наук, професор, професор кафедри теоретичної та комп'ютерної механіки Дніпровського національного університету ім. Олеся Гончара ГАРТ Етері Лаврентіївна*
Адреса: *49010, Україна, м. Дніпро, проспект Гагаріна, 72, Дніпровський національний університет ім. Олеся Гончара*
Мобільний тел.: *+38(050) 146-88-43*
E-mail: hart@ua.fm
ORCID ID: https://orcid.org/0000-0002-6075-2269

Автор (науковий ступень, вчене звання, посада): *аспірант Дніпровського національного університету ім. Олеся Гончара ТЕРЬОХІН Богдан Ігорович*
Адреса: *49010, Україна, м. Дніпро, проспект Гагаріна, 72, Дніпровський національний університет ім. Олеся Гончара*
Мобільний тел.: *+38(095) 072-22-25*
E-mail: bogdan.teryokhin@gmail.com
ORCID ID: https://orcid.org/0000-0003-2381-8190